

RESEARCH ARTICLE

A novel radiopaque tissue marker for soft tissue localization and *in vivo* length and area measurements

Sambit Sahoo^{1,2}, Andrew R. Baker¹, Bong Jae Jun^{1,2}, Ahmet Erdemir¹, Eric T. Ricchetti², Joseph P. Iannotti², Kathleen A. Derwin^{1,2*}

1 Department of Biomedical Engineering, Lerner Research Institute, Cleveland Clinic, Cleveland, Ohio, United States of America, **2** Department of Orthopaedic Surgery, Orthopedic and Rheumatologic Institute, Cleveland Clinic, Cleveland, Ohio, United States of America

* derwink@ccf.org



Abstract

Purpose

The purpose of the study was to describe the characteristics and demonstrate proof-of-concept and clinical use of a barium sulfate infused polypropylene radiopaque tissue marker for soft tissue localization and *in vivo* measurement of lengths and areas.

Methods

Marker mechanical properties were evaluated by tensile tests. Biocompatibility was evaluated following 8–12 weeks' implantation in a pig model. Proof-of-concept of marker application was performed in a human cadaveric shoulder model, and methods for CT imaging and measurement of dimensions were established. Lastly, the method of clinical use of the markers was described in one patient undergoing arthroscopic rotator cuff repair (RCR).

Results

The radiopaque markers had a tensile strength of 28 ± 4.7 N and were associated with minimal to mild inflammatory tissue reaction similar to polypropylene control. CT-based measurements showed relatively high precisions for lengths (0.66 mm), areas (6.97 mm^2), and humeral orientation angles (2.1°) in the cadaveric model, and demonstrated 19 ± 3 mm medio-lateral tendon retraction and $227 \pm 3 \text{ mm}^2$ increase in tendon area in the patient during 26 weeks following RCR. No radiographic leaching, calcification or local adverse events were observed.

Conclusions

The radiopaque tissue marker was biocompatible and had adequate strength for handling and affixation to soft tissues using standard suturing techniques. The marker could be used with low-dose, sequential CT imaging to quantitatively measure rotator cuff tendon retractions with clinically acceptable accuracy. We envision the radiopaque tissue marker to be

OPEN ACCESS

Citation: Sahoo S, Baker AR, Jun BJ, Erdemir A, Ricchetti ET, Iannotti JP, et al. (2019) A novel radiopaque tissue marker for soft tissue localization and *in vivo* length and area measurements. PLoS ONE 14(10): e0224244. <https://doi.org/10.1371/journal.pone.0224244>

Editor: Guillem Pratz, Stanford University School of Medicine, UNITED STATES

Received: June 21, 2019

Accepted: October 8, 2019

Published: October 18, 2019

Copyright: © 2019 Sahoo et al. This is an open access article distributed under the terms of the [Creative Commons Attribution License](https://creativecommons.org/licenses/by/4.0/), which permits unrestricted use, distribution, and reproduction in any medium, provided the original author and source are credited.

Data Availability Statement: All relevant data are within the manuscript.

Funding: Research reported in this publication was supported in part by the Cleveland Clinic Department of Orthopaedics Shoulder Research Fund, the Cleveland Clinic Orthopaedic Operating Room of the Future program, and the National Institute of Arthritis and Musculoskeletal and Skin Diseases of the National Institutes of Health under Award Number 5R01AR068342 to JPI and KAD. The content is solely the responsibility of the

authors and does not necessarily represent the official views of the National Institutes of Health. The funders had no role in study design, data collection and analysis, decision to publish, or preparation of the manuscript.

Competing interests: SS, ARB, KAD, and JPI receive royalties and have a pending patent application related to the FibermarX™ radiopaque tissue marker licensed by Cleveland Clinic to Viscus Biologics, LLC. This does not alter our adherence to PLOS ONE policies on sharing data and materials.

useful for soft tissue localization and *in vivo* measurement of tissue and organ dimensions following surgery.

Introduction

Accurate and repeatable techniques for radiographic localization and *in vivo* measurement of the dimensions of tissues and organs are desirable in various surgical disciplines. Implantable radiopaque markers have been used in orthopedic applications to monitor the healing/failure of tendon and ligament repairs [1–6]. In particular, radiopaque marker tracking using three-dimensional (3D) X-ray imaging techniques such as radiostereometric analysis (RSA) and computed tomography (CT) has been used to monitor anterior cruciate ligament (ACL) graft stretching and migration [1], stiffness of healing Achilles tendon repairs [2], and length across rotator cuff repairs (RCR) to indicate healing/failure after surgery [3–6]. These techniques permit soft tissue measurements with accuracy <1 mm [1, 7, 8]. Implanted radiopaque markers have also been used to reconstruct the 3D geometry of the heart and track movements of the heart wall [9–11]. Implanted radiopaque markers have also been used during radiotherapy planning and image-guided treatment to locate tumor margins and internal organ movement in tumors of the prostate [12–15], uterine cervix [16], lung [17], liver, and spinal/paraspinal lesions [18].

A review of the literature reveals that all prior studies [9–18] used metal-based radiopaque tissue markers made from tantalum, platinum, gold, or stainless steel in the form of spherical beads (~0.8–1.6 mm diameter), rods, rings, or sutures. The use of metal markers has been known to be associated with the risk of breakage [5] and migration within soft tissues [3, 8]. Such markers often therefore require securing by a secondary means such as suture fixation [19–22]. While feasible, affixing metal markers to tissues with suture is technically challenging and time-consuming and therefore not broadly applicable outside of the research setting. Hence, an implantable non-metallic radiopaque marker that can be readily affixed to tissues with minimal time or technical burden and allows accurate localization and length measurements would be desirable for radiographic localization and *in vivo* measurement of tissue and organ dimensions in potentially a broad range of surgical applications.

To address this need, we have developed a radiopaque tissue marker that can be readily tied to body tissues during surgical procedures to allow radiographic visualization of the target locations. We have previously demonstrated the application of this marker in a porcine hernia model, wherein the marker was used to objectively assess and quantify hernia formation, localize mesh implants and monitor hernia size and volume using longitudinal CT imaging [23, 24]. In this manuscript, we describe the mechanical properties, biocompatibility and sub-chronic toxicity, proof-of-concept and finally clinical use of the radiopaque tissue marker for soft tissue localization and measurement of tendon retraction following rotator cuff repair. We hypothesize that the radiopaque tissue marker can be readily affixed to rotator cuff tendon using arthroscopic technique and used with CT imaging to quantitatively measure tendon retraction following rotator cuff repair.

Materials and methods

Radiopaque tissue marker

The radiopaque tissue marker (FibermarX™, Viscus Biologics LLC, Cleveland, OH) is a sterile, USP size-0 polypropylene monofilament infused with barium sulfate. The marker is visible on

standard radiographs (e.g., X-ray, mammography, CT) and has been cleared by the US Food and Drug Administration (FDA) for use during open, percutaneous, or arthroscopic/ laparoscopic/ endoscopic procedures to radiographically mark a soft tissue location during a surgical procedure or for future surgical procedures (510(k), K170026).[25]

Mechanical properties

Tensile tests were conducted using a material testing machine (MTS 858, MTS systems, Eden Prairie, MN) equipped with a 100 lb (~45 kg) load cell affixed to a Capstan fixture following the ASTM D 2256–02 specifications.[26] Segments of the radiopaque marker (30 cm long, $n = 3$) were affixed to the Capstan fixture and pulled at a constant rate of 30 cm/min until failure. For comparison, segments of USP size-0, 2–0, and 3–0 polypropylene (Prolene™, Ethicon) were also tested as a non-barium sulfate loaded, polypropylene controls ($n = 3/$ group). The breaking strength (maximum load attained by specimen prior to failure) and percent elongation (maximum elongation of the suture divided by the initial gage length, 22.6cm) were determined.

Biocompatibility and sub-chronic toxicity

Biocompatibility and sub-chronic toxicity of the radiopaque marker were evaluated following 8 and 12 weeks of implantation in the abdominal wall of two female Yorkshire pigs (30–40kg, 3–4 months old, Michael Fanning Farms, Howe, IN) that were part of a separate study investigating hernia repair [23, 24]. At the time of hernia surgery, the radiopaque marker and USP size 2–0 Prolene™ markers (as a non-barium sulfate loaded, polypropylene control) were applied on the rectus abdominal musculofascial layer remote to the hernia repair site as interrupted simple sutures secured with a knot with four alternating half-hitches. All animal experiments complied with the National Institutes of Health guide for the care and use of Laboratory animals [27] and were approved by the Institutional Animal Care and Use Committee at the Cleveland Clinic (Approval # ARC 2014–1307). The NC3Rs ARRIVE Guidelines checklist is presented in the [S1 Checklist](#).

Postoperative analgesia was provided by the Fentanyl transdermal patch (50 µg/h, applied pre-operatively), IM buprenorphine (0.005–0.01 mg/kg, 2 doses on day of surgery) and IM meloxicam (5mg OD on day of surgery and the day after, if required). All animals were monitored for postoperative complications during the 12 week course of the study.

Following 8 and 12 week of implantation, the animals (one at each time-point) were anaesthetized using IM ketamine (20 mg/kg) and xylazine (2 mg/kg), and euthanized (0.2ml/kg Beuthanasia, I.V.; Intervet/Merck Animal Health, Madison, NJ). The abdomen was opened and tissue strips containing the radiopaque marker and 2–0 Prolene were harvested, fixed in 10% neutral buffered formalin and processed for routine paraffin embedding and histology. After hematoxylin and eosin (H&E) staining, the histology sections were scanned in their entirety at 20X using a Leica SCN400F scanner (Leica Microsystems, GmbH, Wetzlar, Germany). Representative sections from each animal were descriptively reviewed and assessed for biocompatibility and sub-chronic toxicity by a board-certified pathologist.

Proof-of-concept assessment in a cadaveric shoulder rotator cuff model

To assess the feasibility for clinical use in rotator cuff repair patients, the radiopaque marker was next evaluated in a human cadaveric shoulder model to demonstrate proof-of-concept of marker application, and establish the methods for CT imaging and analysis. A full upper extremity and shoulder girdle from a 75-year-old female donor (Anatomic Gifts Registry, Hanover, MD) was used. The cadaver donor was not from a vulnerable population and the

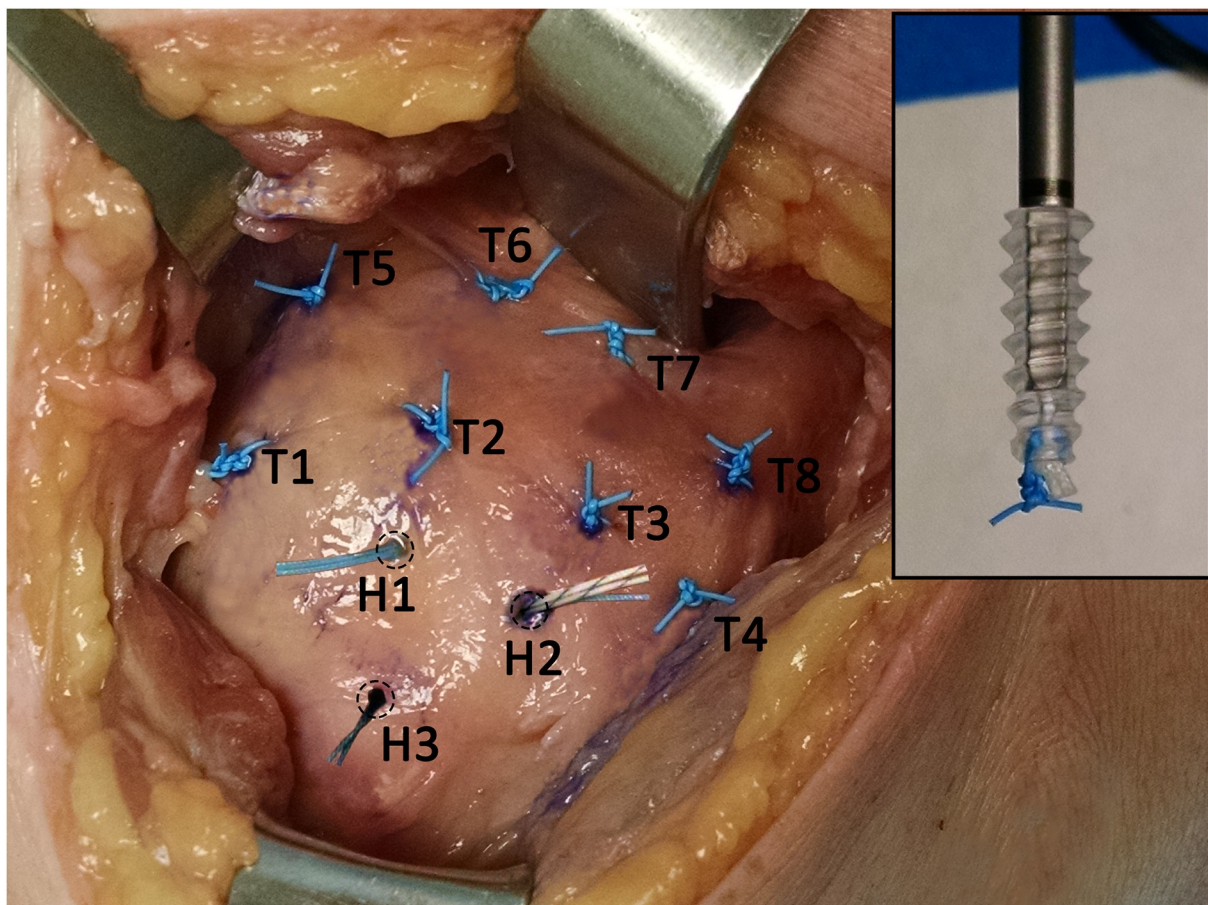


Fig 1. Eight radiopaque tissue markers were secured on the rotator cuff tendons (T1-T8). Three additional markers were tied to the distal tip of suture-anchors (inset) which were secured into the humerus (H1-H3) through the rotator cuff footprint.

<https://doi.org/10.1371/journal.pone.0224244.g001>

donor or next of kin provided written informed consent that was freely given. The bursal surface of the rotator cuff tendons was exposed incising and retracting the skin and deltoid muscle. After removing any loose bursal tissue to clearly identify the rotator cuff tendons, eight radiopaque markers were applied on the bursal surface of the tendons (T1-T8) as interrupted simple sutures secured with a knot with four alternating half-hitches (Fig 1). The first row of four markers (T1-T4) were placed approximately 1.5 cm from the lateral edge of the tendon footprint, and the second row of four markers (T5-T8) were placed approximately 1 cm medial to the first row. Next, three bone markers (H1-H3) were placed by tying a radiopaque marker knot stack to the distal tip of three bone anchors (Arthrex, BioComposite Corkscrew[®] FT suture anchors, 5.5 mm) (Fig 1, inset). These anchors were subsequently secured into the humerus at the rotator cuff footprint. Next, the deltoid was repositioned and the skin was closed in layers using routine surgical techniques.

The cadaver shoulder was approximated to a neutral position, and imaged on a Siemens SOMATOM Definition Edge scanner having 64 detectors with 128 channels. A low-dose CT protocol (100 kV, 45 mAs, 0.6 mm collimation width; CTDIvol 1.8 mGy) was used to scan the entire specimen. The specimen was then removed from the CT scanner, manipulated and re-approximated to the neutral position, and imaged. This was repeated to obtain a total of three scans for the specimen.

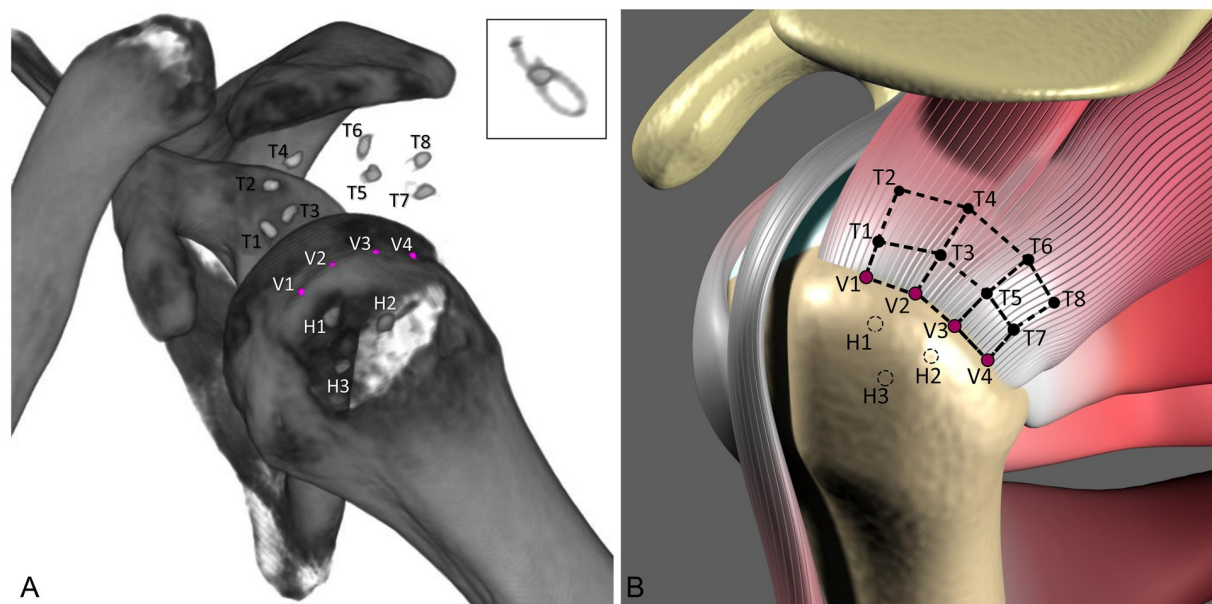


Fig 2. (A) CT image of a human cadaver shoulder obtained using a low dose scan protocol (100 kV, 45 mAs, CTDIvol of 1.8 mGy, 0.6mm collimation width), and (B) a schematic showing the locations of the radiopaque markers on the rotator cuff tendons (T1-T8) and in the humerus (H1-H3). Four virtual markers were placed on the rotator cuff footprint during image analysis (pink, V1-V4). While the radiopaque marker knot stacks were used to localize the tendon and bone markers, single strands of the marker could also be visualized (inset in A). The 3D coordinates of the tendon and virtual markers were used to calculate select lengths and areas.

<https://doi.org/10.1371/journal.pone.0224244.g002>

Image reconstruction was performed using B40F (soft tissue) convolution kernels without overlap or dose modulation, using a field of view (FOV) of 25.6 cm, and slice-thicknesses of 0.6mm. The CT image sets were analyzed using custom-written image analysis software to determine clinically relevant tendon lengths, areas and humeral orientation. First, the scapular [28–30] and humeral coordinate systems were defined by bony landmarks on the scapula and humerus, respectively, and positive direction was assigned to anterior, superior, and lateral, pointing outward. Next, the eight tendon markers (T1–T8) and three humeral bone markers (H1–H3) were identified by the analyst using the software. The software fit each tissue marker to the volumetric centroid of the voxels identified as a marker. Additionally, four “virtual” bone markers (V1–V4, Fig 2A and 2B) were placed along the lateral edge of the rotator cuff footprint by the analyst, to allow clinically-relevant measurements of displacement of tendon markers with respect to the rotator cuff tendon insertion into the bone.

The 3D coordinates of the tendon, humeral and virtual bone markers computed by the software were analyzed using custom MATLAB code (Mathworks, Natick, MA) to calculate select lengths and the areas enclosed by the FiberMarX™ marker array (Fig 2B). Briefly, lengths were defined as the Euclidean distance (straight line distance) between markers, and the areas of the quadrilaterals formed by sets of four markers were approximated by determining the sum of the areas of piecewise triangles, i.e., for each triangle using the one half of the magnitude of the cross-product of vectors forming the two edges of the triangle. The area calculation was performed twice and averaged, by swapping the triangulation.

Additionally, humeral orientations relative to the scapular coordinate system were also calculated. Abduction/adduction was defined by the projected angle to the coronal plane between the superior-inferior axes of the humerus and the scapula. Internal/external rotation was defined by the projected angle to the axial plane between the medial-lateral axes of the humerus and the scapula. Flexion/extension was defined by the projected angle to the sagittal

plane between the superior-inferior axes of the humerus and the scapula. The mean and standard deviation of lengths, areas and humeral orientation angles were measured for the three repeat scans. The precision of measurements for lengths, areas and humeral orientation angles was estimated by averaging the standard deviations of the respective measures (14 lengths, 6 areas, and 3 angles).

Radiopaque marker use in patients with rotator cuff repair

The radiopaque marker is currently being used in a prospective clinical study investigating the natural history of healing following arthroscopic rotator cuff repair [31]. 125 patients between 18–75 years, having a 1–5 cm tear of their supraspinatus and/or infraspinatus tendons that is fully repairable by a double row technique, are included in this study conducted under the approval of the Cleveland Clinic Institutional Review Board (Approval # 16–089). Herein, the method of use of the radiopaque marker and preliminary results of CT analysis from one patient (66 year old, female, 2.5 cm tear in supraspinatus tendon) is described to demonstrate proof-of-concept in an *in vivo* setting.

During the tendon repair for this patient, three tantalum beads were introduced into the bone anchor holes just prior to insertion of the anchors, and these serve as the bone markers (H1, H2, H3). Tantalum beads were used as bone markers because the radiopaque marker is currently FDA-cleared only for marking “soft tissue during a surgical procedure or for future surgical procedures” (510(k), K170026).[25] Following tendon repair, four radiopaque markers were tied to the superficial surface of their tendon just medial to the repair sutures at approximately 0.5-1cm intervals in the anterior-posterior direction, using a standard suture lasso and arthroscopic knot tying technique (T1, T3, T5, and T7). The full grid of tendon markers used to demonstrate proof-of-concept in the cadaver study is not used in the clinical study. Multiple postoperative outcomes were measured, but in particular, this patient underwent low-dose CT imaging (100 kV, 45 mAs, 0.6 mm collimation width; 1.8 mGy CTDIvol) at day of surgery, 3 weeks, 12 weeks, and 26 weeks postoperatively to measure tendon retraction using the implanted radiopaque markers. For CT scanning, patients were supine with the affected arm at the side in neutral rotation, and hand on the thigh; the unaffected arm was extended over the head.

The longitudinal CT image sets from the patient were then analyzed by the software described in the previous section to evaluate changes in tendon lengths, areas and humeral orientation over time. The follow-up CT image sets were imported into the software and registered with respect to the scapula from the day of surgery CT image set. For each CT image set, the tendon markers and humeral bone markers were identified and defined by the analyst, and the software computed their 3D coordinates. The coordinates of the four virtual bone markers (V1-V4) are directly imputed from their rigid body relationship to the humeral bone markers established in the reference CT image set. Tendon lengths, areas and humeral orientation are then calculated as described in the previous section, to assess their change over time.

Results

Mechanical properties

The radiopaque marker had a tensile strength of 28 ± 4.7 N and an elongation at break of $19 \pm 3.7\%$. Similar gage USP size-0 Prolene™ had a tensile strength of 56 ± 0.6 N and an elongation at break of $27 \pm 0.2\%$. The mechanical properties of USP size 2–0 and 3–0 Prolene™ are also reported for comparison (Table 1).

Table 1. Mechanical properties of the radiopaque marker (FibermarX™) and non-radiopaque polypropylene (n = 3/group).

	FibermarX™	0 Prolene™	2–0 Prolene™	3–0 Prolene™
Tensile Strength (N)	28 ±4.7	56 ±0.6	42 ±1.6	23 ±0.2
Extension at break (%)	19 ±3.7	27 ±0.2	25 ±2.8	31 ±0.5

<https://doi.org/10.1371/journal.pone.0224244.t001>

Biocompatibility and sub-chronic toxicity

No difference was observed between the host tissue response to the radiopaque marker and 2–0 Prolene™ suture (control) following implantation in the porcine ventral abdominal wall for 12 weeks (Fig 3). The inflammatory cells around the radiopaque marker and Prolene™ suture consisted primarily of lymphocytes and macrophages with occasional multinucleated giant cells; eosinophils were absent.

Feasibility assessment in cadaveric shoulder rotator cuff model

The radiopaque tissue markers could be readily affixed at the desired locations on the rotator cuff tendon in the human cadaver model using standard open suturing techniques. The

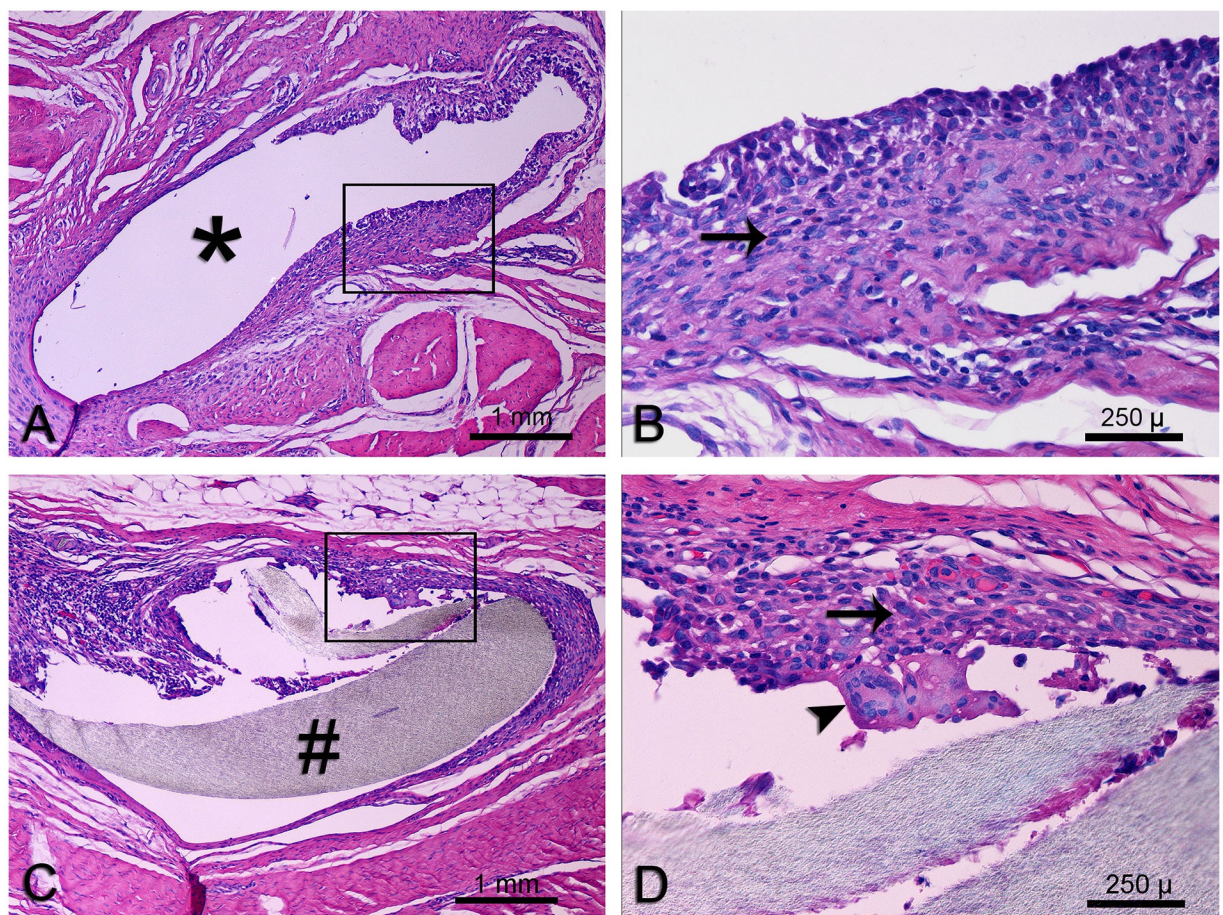


Fig 3. Photomicrographs of representative hematoxylin and eosin-stained sections of the host tissue response to 2–0 Prolene™ suture (A, B) and the radiopaque marker (C, D). B and D represent magnified views of the boxed region in A and C respectively; location of 2–0 Prolene™ suture (*), radiopaque marker (#), lymphocytes and macrophages (arrows), and a multinucleated giant cell (arrowhead). No difference was observed between the host tissue response to the radiopaque marker and 2–0 Prolene™ suture (control).

<https://doi.org/10.1371/journal.pone.0224244.g003>

Table 2. Measurements of tendon lengths, areas, and humeral orientation in the cadaveric shoulder rotator cuff model. Data are presented as mean ± standard deviation (SD) of measurements made from three CT scans repeated after manual manipulation and repositioning of the specimen.

Measurement variable		Mean ± SD	Precision
Tendon, mediolateral lengths (mm)	V1T1	13.2 ± 0.59	0.66
	T1T2	10.0 ± 0.93	
	V2T3	12.6 ± 0.82	
	T3T4	18.2 ± 0.69	
	V3T5	14.0 ± 0.45	
	T5T6	12.0 ± 0.65	
	V4T7	12.4 ± 0.71	
	T7T8	10.7 ± 0.42	
Tendon, antero-posterior lengths (mm)	T1T3	4.4 ± 0.60	6.97
	T3T5	18.3 ± 0.55	
	T5T7	11.5 ± 0.39	
	T2T4	9.6 ± 0.93	
	T4T6	13.3 ± 0.86	
	T6T8	12.0 ± 0.72	
Tendon marker areas (mm ²)	V1V2T3T1	71.2 ± 1.81	6.97
	T1T2T3T4	61.2 ± 5.56	
	V2V3T5T3	168.6 ± 5.74	
	T3T5T6T4	215.5 ± 19.64	
	V3V4T7T5	126.0 ± 4.17	
	T5T7T8T6	129.7 ± 4.88	
Humeral orientation (degrees)	Extension	16 ± 2.1	2.1
	External rotation	14 ± 0.9	
	Abduction	22 ± 3.3	

<https://doi.org/10.1371/journal.pone.0224244.t002>

4-throw knot portion of the marker was prominent and used for localization by CT image analysis, however, the single pass of the radiopaque marker through the tissue at each tendon location was also readily visualized. As a demonstration of proof-of-concept of using the method for quantitative measurements, select tendon lengths (n = 14) and areas (n = 6) enclosed by the radiopaque tissue marker array, as well as the humeral orientation angles from three CT scans are reported in Table 2. Tendon lengths ranged from 4.4 to 18.3 mm, tendon areas ranged from 61.2 to 215.5 mm², and humeral orientation angles ranged from 14° to 22°. The precision of measurements was 0.66 mm for tendon lengths, 6.97 mm² for tendon areas, and 2.1° for humeral orientation angles.

Clinical application in rotator cuff repair patients

The radiopaque tissue markers could be readily affixed intraoperatively at the desired locations on the repaired rotator cuff using standard arthroscopic suturing techniques. No local adverse events were observed in the patient during 26 weeks of follow-up. The knotted portion of the markers was prominent at all time-points, with no evidence of barium leaching or calcification around the markers. Since four lateral row tendon markers were applied in this patient, four medio-lateral tendon lengths, three antero-posterior tendon lengths and three tendon areas enclosed by the radiopaque marker array were calculated, in addition to the humeral orientation angles at the different time-points (Table 3). Fig 4 illustrates the changes in medio-lateral lengths and areas on the rotator cuff tendon during 26 weeks following repair. The

Table 3. Measurements of select lengths and areas on the rotator cuff tendon, and humeral orientation angles in a patient during 26 weeks following arthroscopic rotator cuff repair.

	Variable	0 week	3 week	12 week	26 week
Tendon, mediolateral distances (mm)	V1T1	11.0	16.3	23.3	29.4
	V2T3	17.5	20.9	32.7	40.8
	V3T5	23.9	26.7	36.3	41.5
	V4T7	21.5	23.0	33.6	38.5
Tendon, antero-posterior lengths (mm)	T1T3	7.5	9.5	12.2	14.1
	T3T5	12.4	13.2	12.7	11.4
	T5T7	9.0	11.1	14.6	12.9
Tendon marker areas (mm ²)	V1V2T3T1	119.9	181.2	288.9	384.2
	V2V3T5T3	204.2	250.6	363.6	411.6
	V3V4T7T5	205.7	248.0	389.0	413.7
Humeral orientation (degrees)	Extension	2.3	4.6	2.0	4.0
	External rotation	28.4	56.4	59.1	56.9
	Abduction	17.2	9.0	5.2	0.3

<https://doi.org/10.1371/journal.pone.0224244.t003>

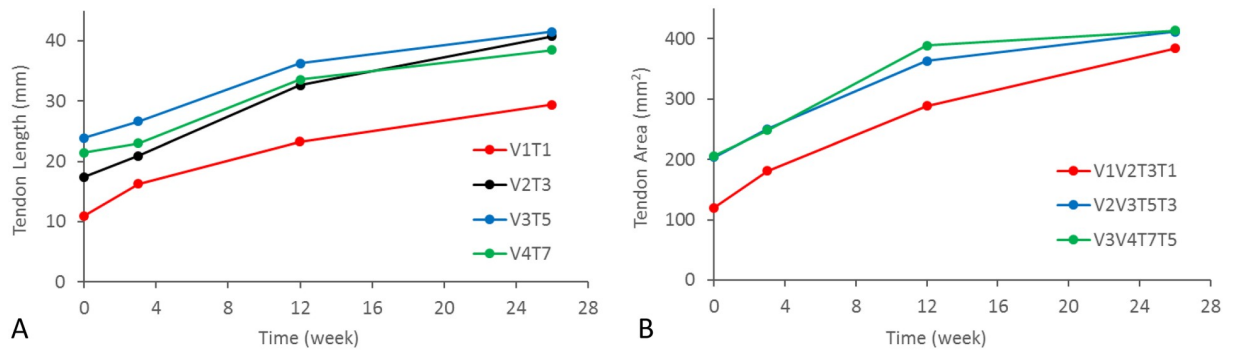


Fig 4. Results from longitudinal analysis of CT data from one patient, for demonstrative purposes, depict an increase in (A) medio-lateral lengths (V1T1, V2T3, V3T5, and V3T7) and (B) areas (V1V2T3T1, V2V3T5T3, and V3V4T7T5) across the rotator cuff tendon repair over 26 weeks post-operation.

<https://doi.org/10.1371/journal.pone.0224244.g004>

interpretation of this finding is part of our ongoing study with the full 125-patient cohort, being followed out to 2 years post-operation.

Discussion

The purpose of the current study was to describe a radiopaque tissue marker—its mechanical properties, biocompatibility and sub-chronic toxicity, proof-of-concept and finally clinical use for soft tissue localization and measurement in the context of rotator cuff repair. The results of the study demonstrate that the radiopaque marker possesses adequate handling characteristics and mechanical properties to readily allow fixation to tissues using standard open and arthroscopic knot-tying tools and techniques. Tensile properties of the radiopaque marker were comparable to 2–0 and 3–0 Prolene. The radiopaque marker also demonstrated biocompatibility and sub-chronic toxicity similar to polypropylene without barium sulfate; such minimal to mild inflammatory tissue reaction to implanted polypropylene has been reported in several studies, and suggests that barium sulfate in the radiopaque marker did not affect host response.

No radiographic leaching, calcification or other significant local adverse events were observed following marker implantation.

Radiopaque markers implanted on the rotator cuff tendon and in the humerus (in the cadaver study) could be readily visualized under low-dose CT. Custom image analysis software was developed for registration of multiple CT image sets, definition of anatomic coordinate systems, placement of virtual markers, and computation of radiopaque marker locations and humeral rotation angles. In particular, software-generated “virtual” markers could be placed at anatomically relevant but otherwise technically challenging or even impossible physical locations. Virtual bone makers placed along the rotator cuff tendon footprint allow measurement of displacement of tendon-markers with respect to tendon footprint (e.g., V1T1), could provide information on tendon gapping or stretching at various locations along a repair/re-tear. Similarly, distance across the lateral row of tendon markers (T1T3 + T3T5 + T5T7) could provide information on the antero-posterior width of a repair/re-tear, and the area enclosed by the virtual and lateral tendon markers (V1V2T3T1 + V2V3T5T3 + V3V4T7T5) could provide information about the size of a repair/re-tear.

The cadaveric shoulder study showed that measurements using the radiopaque markers could be made with a precision of 0.66 mm for tendon lengths, 6.97 mm² for areas, and 2.1° for humeral orientation angles. These values were relatively small compared to the respective absolute measures for this application (5–6% for lengths and areas, and 12% for humeral angles). In particular, the precision of length measurement was in the order of the marker size (~1mm knot diameter) and the resolution of the CT scanner (0.5 mm x 0.5 mm x 0.6 mm resolution), and would be considered acceptable for measuring rotator cuff tendon retraction after repair, which is on the order of centimeters¹⁰. Indeed, longitudinal data from the rotator cuff repair patient included for demonstrative purposes showed that medio-lateral lengths across the tendon repair (i.e., tendon retraction) increased 19 ± 3 mm during 26 weeks post-operation. Concomitantly, areas across the rotator cuff tendon repair increased 227 ± 3 mm² during 26 weeks following repair.

Qualitative variability in arm position was shown to introduce ± 3 mm of spurious variation in length measurements between rotator cuff tendon and bone markers [7]. Now to quantify variance in humeral orientation across multiple scans in a subject with the goal to possibly control for the associated measurement error, we designed our custom software to allow precise computation of humeral orientation with respect to the scapula. As expected, there was minimal variation in humeral orientation in the cadaver specimen that could be easily re-positioned between scans. In the clinical study, though attempts were made to consistently position the patient’s arm in a similar position during follow-up imaging, humeral orientation, particularly external rotation angle, was observed to vary as much as ~30° among scans in this patient. We will evaluate the influence of variation in arm position on error introduced in tendon length and area measurements as sufficient data becomes available in our ongoing patient cohort.[31]

The radiopaque tissue marker was developed to reduce technical challenges and risks associated with steel sutures [4–6] and tantalum beads [3, 8] that have previously been used for marking soft tissues. Affixing the steel suture/ tantalum bead markers to soft tissues is technically challenging and carries the risk of steel suture fragmentation [5], bead detachment and dislocation from the target site [3, 8]. While the current study demonstrated the utility of the radiopaque marker in rotator cuff repair, the marker could have several other applications and be placed on target tissues/organs through an open, percutaneous or endoscopic approach. For example, we have previously demonstrated that the radiopaque marker could be used to mark a ventral hernia defect as well as an implanted hernia mesh to monitor the change in defect size, mesh size, and hernia bulging using longitudinal CT scans in a porcine hernia

repair model [23, 24]. We also envision the radiopaque markers could have application in other musculoskeletal surgical procedures like ACL or Achilles tendon repair or repair of the soft tissues following joint arthroplasty. Additionally we envision that the radiopaque marker could be used in marking a biopsy location or tumor resection bed, in tumor localization and monitoring tumor resection margins, in breast imaging, or vessel anastomosis. In addition to exploring the use of the radiopaque marker in a variety of applications, the potential utility of using the radiopaque tissue markers with dynamic imaging modalities such as biplanar radiography or RSA to assess joint kinematics [32, 33] or tissue strain [4, 5] should be assessed in future work.

The study's objective was to demonstrate the proof-of-concept of using a radiopaque marker for visualization and measurement following surgical implantation. The marker is biocompatible and can be visualized under low-dose CT imaging (CTDIvol: 1.8 mGy/scan; effective dose: 1.0 mSv/scan). The health risks from radiation exposure of this magnitude are extremely small with no identifiable additional cancer risk [34, 35]. The patient example provided here demonstrates how software-based marker analysis of CT scans can allow for clinically relevant measurements to be made from the implanted markers, which in some applications may enhance the clinical utility of the markers over simple visual inspection. However, the marker is also readily visualized by standard planar X-ray and mammography as well as if radiographic visualization is all that is desired; the marker is visible on planar X-rays, even at viewing angles where it overlaps with bony structures, although it does have lower contrast compared to traditional tantalum markers.

Conclusions

In summary, we report on a radiopaque tissue marker that could be readily affixed to tissues and implants and visualized under low-dose CT imaging. The marker is biocompatible and stable over time following implantation. Longitudinal CT image analysis of the radiopaque marker array implanted on the repaired rotator cuff could quantify variations in arm position and provide clinically-relevant length and area measurements with acceptable accuracy for measuring tendon retraction. We envision the radiopaque tissue markers to be useful for soft tissue localization and *in vivo* measurement of tissue and organ dimensions in potentially a broad range of surgical applications.

Supporting information

S1 Checklist. NC3Rs ARRIVE Guidelines checklist.
(PDF)

Acknowledgments

We acknowledge the Imaging Institute at Cleveland Clinic for generous donation of acquisition time on the Siemens SOMATOM Definition Edge clinical scanner, and Tracy Painter, CT Clinical Manager, for technical assistance in performing the CT scans.

Author Contributions

Conceptualization: Sambit Sahoo, Kathleen A. Derwin.

Data curation: Sambit Sahoo, Andrew R. Baker.

Formal analysis: Sambit Sahoo, Andrew R. Baker, Bong Jae Jun, Ahmet Erdemir.

Funding acquisition: Joseph P. Iannotti, Kathleen A. Derwin.

Investigation: Sambit Sahoo, Joseph P. Iannotti, Kathleen A. Derwin.

Methodology: Sambit Sahoo, Bong Jae Jun, Ahmet Erdemir, Eric T. Ricchetti, Joseph P. Iannotti, Kathleen A. Derwin.

Project administration: Sambit Sahoo, Kathleen A. Derwin.

Resources: Sambit Sahoo, Kathleen A. Derwin.

Supervision: Kathleen A. Derwin.

Validation: Sambit Sahoo, Eric T. Ricchetti, Joseph P. Iannotti.

Visualization: Sambit Sahoo.

Writing – original draft: Sambit Sahoo.

Writing – review & editing: Sambit Sahoo, Andrew R. Baker, Bong Jae Jun, Ahmet Erdemir, Eric T. Ricchetti, Joseph P. Iannotti, Kathleen A. Derwin.

References

1. Khan R, Konyves A, Rama KR, Thomas R, Amis AA. RSA can measure ACL graft stretching and migration: development of a new method. *Clin Orthop Relat Res.* 2006; 448:139–45. Epub 2006/07/11. <https://doi.org/10.1097/01.blo.0000224016.42669.17> PMID: 16826108.
2. Schepull T, Kvist J, Andersson C, Aspenberg P. Mechanical properties during healing of Achilles tendon ruptures to predict final outcome: a pilot Roentgen stereophotogrammetric analysis in 10 patients. *BMC musculoskeletal disorders.* 2007; 8(Journal Article):116. Epub 2007/11/28. <https://doi.org/10.1186/1471-2474-8-116> PMID: 18039357.
3. McCarron JA, Derwin KA, Bey MJ, Polster JM, Schils JP, Ricchetti ET, et al. Failure with continuity in rotator cuff repair "healing". *Am J Sports Med.* 2013; 41(1):134–41. Epub 2012/09/29. <https://doi.org/10.1177/0363546512459477> PMID: 23019253.
4. Cashman PM, Baring T, Reilly P, Emery RJ, Amis AA. Measurement of migration of soft tissue by modified Roentgen stereophotogrammetric analysis (RSA): validation of a new technique to monitor rotator cuff tears. *Journal of medical engineering & technology.* 2010; 34(3):159–65. Epub 2010/02/11. <https://doi.org/10.3109/03091900903174428> PMID: 20143960.
5. Baring TK, Cashman PP, Reilly P, Emery RJ, Amis AA. Rotator cuff repair failure in vivo: a radiostereometric measurement study. *J Shoulder Elbow Surg.* 2011; 20(8):1194–9. Epub 2011/07/23. <https://doi.org/10.1016/j.jse.2011.04.010> PMID: 21778073.
6. Bhatia DN, De Beer JF. Metal markers for radiographic visualization of rotator cuff margins: A new technique for radiographic assessment of cuff repair integrity. *Int J Shoulder Surg.* 2013; 7(1):37–9 PMID: 23858295.
7. Derwin KA, Milks RA, Davidson I, Iannotti JP, McCarron JA, Bey MJ. Low-dose CT imaging of radiopaque markers for assessing human rotator cuff repair: accuracy, repeatability and the effect of arm position. *J Biomech.* 2012; 45(3):614–8. <https://doi.org/10.1016/j.jbiomech.2011.11.046> PMID: 22169153.
8. Smith CK, Hull ML, Howell SM. Migration of radio-opaque markers injected into tendon grafts: a study using roentgen stereophotogrammetric analysis (RSA). *J Biomech Eng.* 2005; 127(5):887–90. <https://doi.org/10.1115/1.1992533> PMID: 16248321.
9. Brower RW, Harald J, Meester GT. Direct method for determining regional myocardial shortening after bypass surgery from radiopaque markers in man. *The American journal of cardiology.* 1978; 41(7):1222–9. [https://doi.org/10.1016/0002-9149\(78\)90879-2](https://doi.org/10.1016/0002-9149(78)90879-2) PMID: 307340
10. Garrison J, Ebert W, Jenkins R, Yionoulis S, Malcom H, Heyler G, et al. Measurement of three-dimensional positions and motions of large numbers of spherical radiopaque markers from biplane cineradiograms. *Computers and biomedical research.* 1982; 15(1):76–96. [https://doi.org/10.1016/0010-4809\(82\)90054-4](https://doi.org/10.1016/0010-4809(82)90054-4) PMID: 7060369
11. Niczyporuk MA, Miller DC. Automatic tracking and digitization of multiple radiopaque myocardial markers. *Computers and biomedical research.* 1991; 24(2):129–42. [https://doi.org/10.1016/0010-4809\(91\)90025-r](https://doi.org/10.1016/0010-4809(91)90025-r) PMID: 2036779

12. Crook J, Raymond Y, Salhani D, Yang H, Esche B. Prostate motion during standard radiotherapy as assessed by fiducial markers. *Radiotherapy and Oncology*. 1995; 37(1):35–42. [https://doi.org/10.1016/0167-8140\(95\)01613-I](https://doi.org/10.1016/0167-8140(95)01613-I) PMID: 8539455
13. Balter JM, Lam KL, Sandler HM, Littles JF, Bree RL, Ten Haken RK. Automated localization of the prostate at the time of treatment using implanted radiopaque markers: technical feasibility. *International Journal of Radiation Oncology* Biology* Physics*. 1995; 33(5):1281–6.
14. Litzenberg D, Dawson LA, Sandler H, Sanda MG, McShan DL, Ten Haken RK, et al. Daily prostate targeting using implanted radiopaque markers. *International Journal of Radiation Oncology* Biology* Physics*. 2002; 52(3):699–703.
15. Aubry J-F, Beaulieu L, Girouard L-M, Aubin S, Tremblay D, Laverdière J, et al. Measurements of intrafraction motion and interfraction and intrafraction rotation of prostate by three-dimensional analysis of daily portal imaging with radiopaque markers. *International Journal of Radiation Oncology* Biology* Physics*. 2004; 60(1):30–9.
16. Kaatee RS, Olofsen MJ, Verstraate MB, Quint S, Heijmen BJ. Detection of organ movement in cervix cancer patients using a fluoroscopic electronic portal imaging device and radiopaque markers. *International Journal of Radiation Oncology* Biology* Physics*. 2002; 54(2):576–83.
17. Berbeco RI, Mostafavi H, Sharp GC, Jiang SB. Towards fluoroscopic respiratory gating for lung tumours without radiopaque markers. *Phys Med Biol*. 2005; 50(19):4481. <https://doi.org/10.1088/0031-9155/50/19/004> PMID: 16177484
18. Shirato H, Harada T, Harabayashi T, Hida K, Endo H, Kitamura K, et al. Feasibility of insertion/implantation of 2.0-mm-diameter gold internal fiducial markers for precise setup and real-time tumor tracking in radiotherapy. *International Journal of Radiation Oncology* Biology* Physics*. 2003; 56(1):240–7.
19. Roos PJ, Hull ML, Howell SM. How cyclic loading affects the migration of radio-opaque markers attached to tendon grafts using a new method: a study using roentgen stereophotogrammetric analysis (RSA). *J Biomech Eng*. 2004; 126(1):62–9. <https://doi.org/10.1115/1.1644568> PMID: 15171130.
20. Bey MJ, Kline SK, Baker AR, McCarron JA, Iannotti JP, Derwin KA. Estimation of dynamic, in vivo soft-tissue deformation: experimental technique and application in a canine model of tendon injury and repair. *J Orthop Res*. 2011; 29(6):822–7. Epub 2011/04/27. <https://doi.org/10.1002/jor.21315> PMID: 21520256.
21. Derwin KA, Baker AR, Codsi MJ, Iannotti JP. Assessment of the canine model of rotator cuff injury and repair. *J Shoulder Elbow Surg*. 2007; 16(5 Suppl):S140–8. Epub 2007/06/15. <https://doi.org/10.1016/j.jse.2007.04.002> PMID: 17560802.
22. Marshall NE, Keller RA, Okoroha K, Guest JM, Yu C, Muh S, et al. Radiostereometric Evaluation of Tendon Elongation After Distal Biceps Repair. *Orthop J Sports Med*. 2016; 4(11):2325967116672620. <https://doi.org/10.1177/2325967116672620> PMID: 27928546.
23. Sahoo S, Baker AR, Haskins IN, Krpata DM, Rosen MJ, Derwin KA. Assessment of Human Acellular Dermis Graft in Porcine Models for Ventral Hernia Repair. *Tissue engineering Part C, Methods*. 2017; 23(11):718–27. <https://doi.org/10.1089/ten.TEC.2017.0238> PMID: 28602151.
24. Sahoo S, Baker AR, Haskins IN, Krpata DM, Rosen MJ, Derwin KA. Development of a critical-sized ventral hernia model in the pig. *J Surg Res*. 2017; 210:115–23. <https://doi.org/10.1016/j.jss.2016.10.026> PMID: 28457317.
25. Radiopaque Tissue Marker (K170026) 2017. https://www.accessdata.fda.gov/cdrh_docs/pdf17/K170026.pdf.
26. ASTM D2256-02: Standard Test Method for Tensile Properties of Yarns by the Single-Strand Method. ASTM International, West Conshohocken, PA; 2002, <http://www.astm.org/cgi-bin/resolver.cgi?D2256-02>.
27. Institute of Laboratory Animal Resources (U.S.). Committee on Care and Use of Laboratory Animals. Guide for the care and use of laboratory animals. NIH publication. Bethesda, Md.: U.S. Dept. of Health and Human Services, Public Health Service. p. volumes.
28. Codsi MJ, Bennetts C, Gordiev K, Boeck DM, Kwon Y, Brems J, et al. Normal glenoid vault anatomy and validation of a novel glenoid implant shape. *J Shoulder Elbow Surg*. 2008; 17(3):471–8. Epub 2008/03/11. <https://doi.org/10.1016/j.jse.2007.08.010> PMID: 18328741.
29. Scalise JJ, Codsi MJ, Bryan J, Iannotti JP. The three-dimensional glenoid vault model can estimate normal glenoid version in osteoarthritis. *J Shoulder Elbow Surg*. 2008; 17(3):487–91. Epub 2008/02/20. <https://doi.org/10.1016/j.jse.2007.09.006> PMID: 18282721.
30. Ganapathi A, McCarron JA, Chen X, Iannotti JP. Predicting normal glenoid version from the pathologic scapula: a comparison of 4 methods in 2- and 3-dimensional models. *J Shoulder Elbow Surg*. 2011; 20(2):234–44. Epub 2010/10/12. <https://doi.org/10.1016/j.jse.2010.05.024> PMID: 20933439.

31. Cleveland Clinic. Rotator Cuff Failure With Continuity (NCT02716441) [updated December 17, 2018]. <https://ClinicalTrials.gov/show/NCT02716441>.
32. Ackland DC, Keynejad F, Pandy MG. Future trends in the use of X-ray fluoroscopy for the measurement and modelling of joint motion. *Proceedings of the Institution of Mechanical Engineers Part H, Journal of engineering in medicine*. 2011; 225(12):1136–48. <https://doi.org/10.1177/0954411911422840> PMID: 22320053.
33. Bey MJ, Zael R, Brock SK, Tashman S. Validation of a new model-based tracking technique for measuring three-dimensional, in vivo glenohumeral joint kinematics. *J Biomech Eng*. 2006; 128(4):604–9. <https://doi.org/10.1115/1.2206199> PMID: 16813452
34. DeMaio DN. CT Radiation Dose and Risk: Fact vs Fiction. *Radiol Technol*. 2017; 89(2):199–205. PMID: 29298927.
35. Lin EC, editor *Radiation risk from medical imaging*. Mayo Clinic Proceedings; 2010: Elsevier.